17th World Conference on Earthquake Engineering, 17WCEE
Sendai, Japan - September 13th to 18th 2020

WHAT IS FLING STEP? – ITS PHYSICS, THEORY, AND STRONG GROUND MOTION SIMULATION NEAR SURFACE FAULT RUPTURE –

Y. Hisada[(1)], S. Tanaka [(2)],

[(1)] *Professor, Department of Architecture, hisada@cc.kogakuin.ac.jp*
[(2)] *Tokyo Electric Power Services Co., Ltd., M. Engineering, s.tanaka@tepsco.co.jp*

Abstract

Fling Step is a displacement waveform like a step function accompanied by a permanent offset appearing in the very vicinity of the surface fault rupture. Despite its importance in Seismological and Engineering field, its physics and theory have been variously interpreted. For example, Ref. [1] interpreted it as "the intermediate term of the elastodynamic equations of motion of Aki and Richards (2002)", whereas Ref. [2] interpreted it as the near field term. Here, the elastodynamic equations are the theoretical solutions of a seismic point source in a homogeneous full-space (Eq. (4.32) in Ref. [3]), where they are separated into the near-, intermediate- and far-field terms.

However, the above interpretations of the fling step are incorrect in the following reasons.

1. The static solutions by a point source are contributed of not only the near-term, but also both the near- and intermediate-terms, as shown in the equation (4.34) in Ref. [3].
2. Because the actual underground structure are complex stratified half-spaces, the theory of a homogeneous full-space is inappropriate.
3. Since the fling step is the result of the elastic rebound very near rupturing surface faults, the theory of the dislocating fault plane should be used, but not a point source. In fact, when an observation point is very close to a fault plane, the amplitudes of seismic waves diverge for a point source, whereas they converge to the value of the fault slip for an extended source (Ref. [4]).

On the other hand, Ref. [4] defined the fling step as "The contribution of static Green function in the representation theorem", which is valid in any underground structures. Based on this definition, we have proposed efficient theoretical simulation methods in layered half-space based on the theoretical wavenumber integration method, and have released Fortran codes for public use (http://kouzou.cc.kogakuin.ac.jp/Open/Green/). In this paper, we show the validity of our definition, and demonstrate various simulation examples using a simple circular fault model and the complex surface faulting model during the 2016 Kumamoto earthquake.

Keywords: Fling Step, Strong Ground Motion Simulation, Surface Fault Rupture, the 2016 Kumamoto earthquake

1. Introduction

Fling Step is displacement waveform including a permanent offset like a step function appearing near the surface fault rupture. Despite its importance in Seismological and Engineering field, its physics and theory have been variously interpreted. For example, Ref. [1] interpreted it as "the intermediate term of the elastodynamic equations of motion of Aki and Richards (2002)", whereas Ref. [2] interpreted it as the near field term. Here, the elastodynamic equations are the theoretical solutions of a seismic point source in a homogeneous full-space (Eq. (4.32) in Ref. [3]), where they are separated into the near-, intermediate- and far-field terms. On the other hand, Ref. [4] defined the fling step as "The contribution of static Green function in the representation theorem". Based on this definition, we have proposed efficient theoretical methods based on the wavenumber integration method in layered half-space for simulating strong ground motions including the fling step effects, and have released Fortran codes for public use. In this paper, we first show the validity of our definition and the physics of the fling step using a simple circular fault model in a homogenous full space. And second, we also demonstrate the validity of our definition using the proposed method in layered half-spaces by simulating the strong motion recorded very near the surface faults during the 2016 Kumamoto earthquake.

2. Theory and Physics of Fling Step in Homogeneous Full-Space

We first show the simplest fling step model by following Ref. [4], that is the analytical solution of the ground motion generated from a circular fault model in the homogeneous full-space. Because of this simplicity, we can separate the solution into the near-, intermediate-, and far-field terms, in addition to the static terms, and investigate which terms contribute the most to the fling step. We also derive the approximate solution of the point source, in addition to the theoretical solution of the circular fault, to demonstrate that the point source solution is inappropriate to simulate the fling step for an observation point very close to the fault plane.

2.1 Analytical solutions of fling step for circular fault in homogeneous full-space

As shown in Fig.1, we derive the analytical solution of the ground motion generated from a circular fault model in the homogeneous full-space. We use a slip function, D, which is uniform over the circular fault of the radius, R, and the observation point is located at a distance, z, above the center of the fault. The displacement wave, U, in the same direction as that of slip, is expressed in Eq. (1) in the frequency domain (Ref. [4]),

$$U_{Fault}(z,\omega) = \frac{zD(\omega)}{4}\int_0^R \frac{r}{\zeta^3}\left\{2u_1(z,\omega)+u_2(z,\omega)\left(\frac{r}{\zeta}\right)^2\right\}dr \qquad (1)$$

where,

$$u_1(z,\omega) = u_1^N + u_1^I + u_1^F \qquad (2\text{-}1)$$

$$u_1^N = \frac{6}{S^2}\left\{(1-S)e^S-(1-P)e^P\right\},$$

$$u_1^I = \frac{1}{S^2}\left(3S^2e^S-2P^2e^P\right), \quad u_1^F = -Se^S$$

$$u_2(z,\omega) = u_2^N + u_2^I + u_2^F \qquad (2\text{-}2)$$

$$u_2^N = -\frac{30}{S^2}\left\{(1-S)e^S-(1-P)e^P\right\},$$

$$u_1^I = -\frac{12}{S^2}\left(S^2e^S-P^2e^P\right), \quad u_1^F = -\frac{2}{S^2}\left(S^3e^S+P^3e^P\right)$$

$$S = i\zeta\omega/\beta, \quad P = i\zeta\omega/\alpha, \quad \zeta = \sqrt{z^2+r^2} \qquad (3)$$

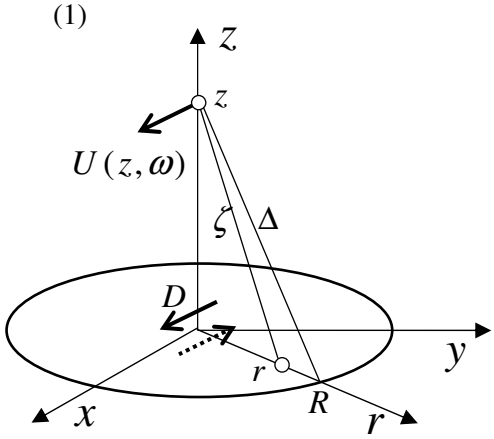

Fig. 1 Circular fault model

The superscripts *N, I, F* in the equations correspond to the terms of the near field, the intermediate, and the far field, respectively. And, α and β are the P-and S-wave velocites, respectively.

The static solutions corresponding to Eqs. (2-1) and (2-2) become as follows using Lopital's theorem.

$$u_1^S = u_1(\omega = 0) = u_1^{NP} + u_1^{IP} = \left(\frac{\beta}{\alpha}\right)^2, \quad u_2^S = u_2(\omega = 0) = u_1^{NS} + u_1^{IS} = 3\left\{1 - \left(\frac{\beta}{\alpha}\right)^2\right\} \tag{4}$$

The superscripts *S* stands for the static contribution. The above equations indicate the static solutions consist of both the near field and intermediate terms, not the far field terms; that conclusion is consistent with the equation (4.34) in Ref. [3].

Substituting Eq. (4) into Eq. (1), we can derive the analytical solution corresponding the static contribution of Green' function of the circular fault model with the slip function D.

$$U_{Fault}^S(z) = \frac{D(\omega)}{4}\left[2 - 3\frac{z}{\Delta} + \left(\frac{z}{\Delta}\right)^3 + \left(\frac{\beta}{\alpha}\right)^2\left\{\frac{z}{\Delta} - \left(\frac{z}{\Delta}\right)^3\right\}\right] \tag{5}$$

where, $\Delta = \sqrt{z^2 + R^2}$. Note that, when an observation point is on the fault plane (z=0), Eq. (5) becomes $U_{Fault}^S = D(\omega)/2$. That is, the displacement waveform on the fault plane is the half of the slip function.

Next, we derive the point source solotions corresponding to Eqs. (1) and (5) as follows, by using $R << z$, and $\Delta \approx \zeta \approx z$.

$$U_{Point}(z,\omega) = \frac{D(\omega)R^2}{4z^2}u_1^F = \frac{M_0(\omega)}{4\pi\rho z^2\beta^2}u_1^F = \frac{\dot{M}_0(\omega)}{4\pi\rho\beta^3 z}e^{i\frac{\omega z}{\beta}} \tag{6}$$

$$U_{Point}^S(z) = \frac{D(\omega)}{4}\left(\frac{\beta}{\alpha}\right)^2\left(\frac{R}{z}\right)^2 = \frac{M_0(\omega)}{4\pi\rho\alpha^2 z^2} \tag{7}$$

where, M_0 ($= \mu DA = \rho\beta^2 D\pi R^2$) and $\dot{M}_0$ ($= -i\omega M_0$) are the functions of the seismic moment and the moment rate, respectivley.

2.2 Comparison of the static amplitudes between a circular fault and a point source

As shown later, since the fling step is the static contribution of Green's function, we demonstrate the difference of the static amplitudes between the circular fault (Eq. (5)) and the point sources (Eq. (7)). Fig.2 shows the relation between the normalized distance (z/R) and the normalized amplitude (U/0.5D). The blue and red lines indicate the solutions of the point source and the circular fault, respectively ($\alpha = 5$ km/s and $\beta = 3$ km/s). When the distance z is larger than the radius R (z/R > 1), the two solutions are identical and show the attenuation of the square of z. On the other hand, when z is less than R (z/R < 1), the amplitude of the point source solution diverges, whereas that of the circular fault converge to one, that is the half of the dislocation (=0.5D). The point source approximation is inappropriate within the distance of the fault radius.

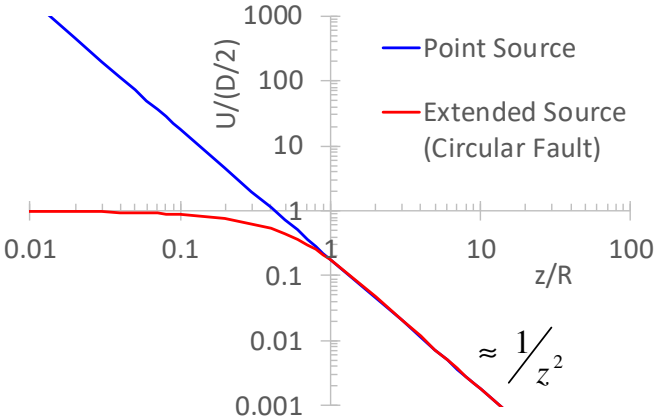

Fig. 2 Comparison of the static amplitude between a circular fault (red line) and a point source (blue line)

2.3 The seismic wave simulation from the circular fault, and the physics of fling step

We simulate the seismic waves using Eqs. (1) and (5), and find out which of the static, near-field, or, intermediate terms is most appropriate to represent the fling step. We use the fault model of R=1,000 m, D= 1m, and its slip velocity is the triangle function of the 1 second duration, the media of $\alpha = 5$ km/s and $\beta = 3$ km/s, and the location of the observation point (OP) at z=10, 100, 1,000, and 10,000 m. Fig.3 shows the simulated velocities (left) and displacements (right) The red "Full Wave" lines correspond to the full wave solution (Eq. (1)), which consist of both the dynamic and static solutions, The black "Static Term" lines are the static solutions (Eq. (5)). The "Dynamic Term" lines are the results of the dynamic contributions subtracting the static solutions from the full wave solution. And the "Near Field", "Intermediate", and "Far-Field" lines are their contributions in the full wave solution using Eq. (2).

When OP is very close to the fault plane, i.e., z=10 m and 100 m, which are 1/100 and 1/10 of the radius, respectively, the results of "Static Term" are almost identical to those of "Full Wave" in both velocities and displacements, and those of "Dynamic Term" are negligible. And, thus, the fling steps, whose amplitudes are about 0.5 m (half of the slip), are completely reproduced by the "Static Term". On the other hand, the results of "Near-Field Term" show larger amplitudes than "Full Wave", and require the minus values of "Intermediate Term".

When z=1,000 m, the same distance to the radius R, the permanent offset of "Full Wave" in the displacement is identical to that of "Static Term". As for the velocity, not only "Static Term", but also "Dynamic Term" contributes greatly to represent "Full Wave". When z=10,000 m, 10 times longer than the radius, the contribution of "Static Term" disappears, and that of "Far Field Term" becomes dominant.

In conclusion, the static term is most appropriate to represent the fling step near the fault plane, but not the near or the intermediate terms.

3. Theoretical Method for Simulating Seismic Waves Including Fling Step in Layered Half-Space, and Its Application to the 2016 Kumamoto Earthquake

We show the theoretical method for efficiently simulation the strong ground motions in the layered half-space including the fling step (Ref. [4]). And we apply it to the strong ground motion records near the surface faults of the 2016 Kumamoto earthquake, and confirm that the fling steps are the static contribution of Green's function.

3.1 Modified representation theorem to efficiently simulate fling step

From the representation theorem in frequency domain showing below, we derive the modified theorem, which effectively simulates the fling step,

$$U_k(Y,\omega) = \int_\Sigma T_{ik}(X,Y,\omega)\left[D_i(X,\omega)\right]d\Sigma \tag{8}$$

where, U_k is the kth component of displacement in the Cartesian coordinate system at an observation point (OP) Y, and X is a source point (SP) on the fault plane Σ. T_{ij} is the traction Green's function, and D_i is the ith component of the fault slip function. In the equation, we use the summation convention for subscript i and k.

Next, we show the modified theorem, which effectively simulate fling step (Ref. [4]).

$$U_k(Y,\omega) = \int_\Sigma \left\{T_{ik}(X,Y,\omega) - T_{ik}^S(X,Y)\right\}\left[D_i(X,\omega)\right]d\Sigma + \int_\Sigma T_{ik}^S(X,Y)\left[D_i(X,\omega)\right]d\Sigma \tag{9}$$

where T_{ij}^S is the static traction Green's function of the layered half-space. In Eq. (9), the first and second terms of the right side are the contributions of the dynamic and static Green's functions, respectively, and the latter represents the fling step. When OP (Y) is very close to the fault plane, Eq. (9) simulate the strong

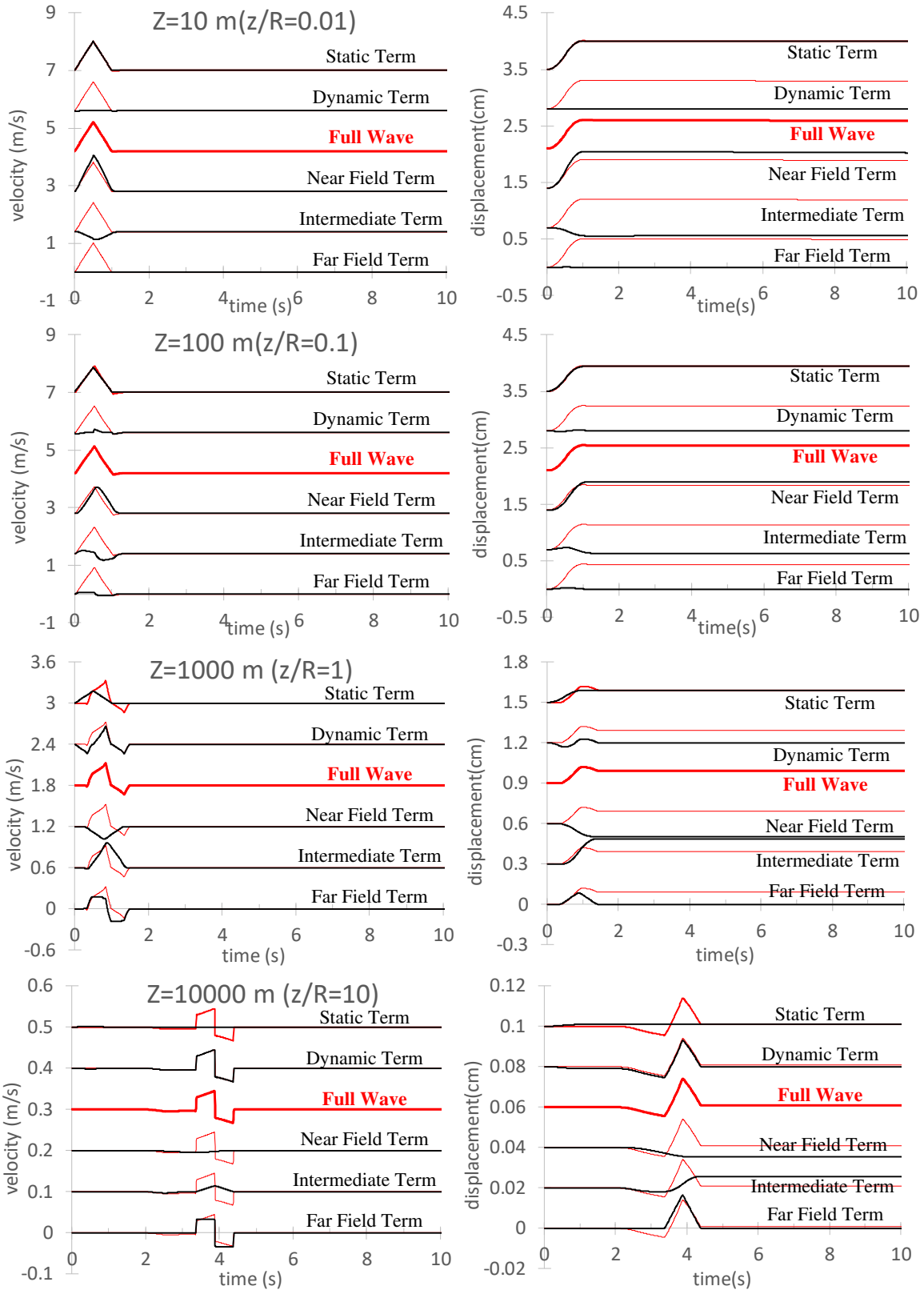

Fig. 3 The seismic waves from the circular fault (the red "full wave" indicate the complete waves, and the static and dynamic terms are their contribuions. And, the near, intermediate, and far field terms are their contributions in the full waves.

ground motions very efficiently, because the singularities of the dynamic Green function for a very close OP to the fault plane are eliminated by subtracting the static Green funcion. And thus, the fault integration can be achieved without any difficulty using regular sub-fault schemes. On the other hand, in the second term of right side in Eq. (9), it is necessary to arrange very dense integration points around SP, according to the proximity between OP and SP. Therefore, the CPU time on the PC is rather time-consuming on this static term, but this is common to all frequencies and only one calculation is needed.

3.2 Fortran77 Code for simulating strong ground motions in layered half-spaces effectively from very near-fault cases including fling step to very far-field cases

Based on the modified representation theorem (Ref. [4]) and the theoretical Green's function of layered half-spaces (Ref. [5]), we have developed Fortran 77 codes for simulating efficiently strong ground motions under any given conditions. And, we have made them open to public use at http://kouzou.cc.kogakuin.ac.jp/Open/Green/. The following are the main features of the code.

1) It carries out high-speed calculation of strong ground motions on a PC under any given conditions from very close to very far from an earthquake fault, and from 0 (static) to very high frequencies. We made it possible by using the theoretical Green's function in a layered half-space based on the wave-number integration method (Ref. [5]). We adopted a) the R/T matrix of the layered half-spaces including the static matrix (Ref. [6])) the dense distribution of wave-number integration points around the singular points (i.e., the pole and branch points), and c) the numerical wave-number integration schemes based on Simpson's and Filon's rules for near- and far sites, respectively.

2) When the depths of SP and OP are very close, such as when SP is on the free surface, the integrands diverse with increasing wave-numbers, making the regular numerical integration schemes impossible. We have solved this problem as follows in Eq. (9). First, in the first term on the right side, we carry out the wave number integration by subtracting the integrand of the static Green function from that of the dynamic Green function. Since the diverging factor of the dynamic Green function is all due to the contribution of the static Green function, the wave number integration can be performed without any problem (Ref. [5]). Next, in the second term, we use the contour deformation method for the wave-number integration, in which the wave numbers on the real axis larger than the largest pole are converted to the imaginary axis by Cauchy's theorem (Ref. [7]). Since the amplitude of the integrand decreases exponentially along the imaginary axis, the numerical integration can be easily performed.

3) It carries out very efficient fault integrations in Eq. (9). When OP is not close to the fault, the area of the fault is divided into sub-faults, and the Gauss - Legendre quadrature is performed using up to 36 points for each sub-fault, which are from 1 to 6 points along the fault length and width directions, respectively. When OP is less than the size of the sub-fault, we use the same fault integration for the first term in Eq. (9), in which the singularities of Green's function are eliminated. On the other hand, for the second term, we repartition the sub-faults repeatedly until all the sub-fault sizes becomes less than the distance from OB to the fault, as shown in Fig.4. And it carries out the Gauss - Legendre quadrature using up to 36 integration points within the subdivided sub-faults.

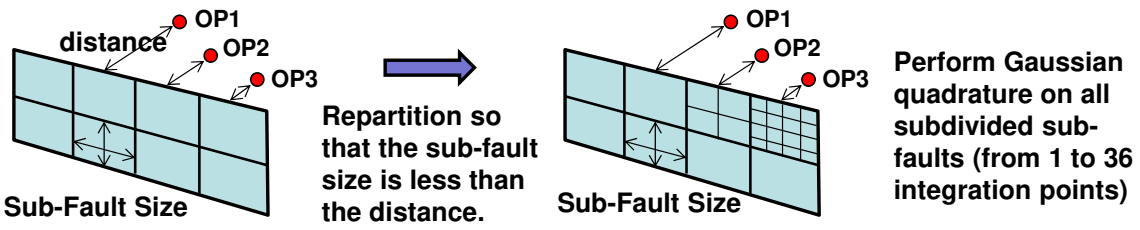

Fig. 4 The fault integration scheme for the observation points close to the fault

3.2 Simulation of the Fling Step during the 2016 Kumamoto Earthquake

Using the Fortran code introduced in the previous section, we simulate the observation records very close to the surface faults ruptured during the 2016 Kumamoto earthquake, and investigate the physics of the recorded fling step.

We simulate the near-fault strong ground motions during the 2016 Kumamoto earthquake (Mw7.0) at periods more than 1 second using the fault model and the layered half-space model with the material properties shown in Fig.5 and Tables 1 and 2 (Ref. [8]). Fig.5(a) shows the location of the Kumamoto earthquake, and Fig. 5(b) shows the two sites, Mashiki and Nishihara, and the three fault models corresponding to the Futagawa, Hinagu, and Idenoguchi faults. The thick solid lines of the fault models correspond to the surface faults, and the dark rectangles correspond to the projections of SMGAs (strong ground motion generation areas). The right figure of Fig.5(c) shows the three fault models; the source parameters for the seismogenic layers (> 3 km depth) are based on the source inversion results (see Ref. [8]), and the recipe of predicting strong ground motions (Ref. [9]). On the other hand, the source parameters for the shallow layers including the surface fault ruptures (< 3 km), we use the extended recipe of predicting strong ground motions (Ref. [8]), in which the empirical smooth slip velocity functions are used. The left figure of Fig.5(c) shows the cross-section including Futagawa and Idenoguchi faults and the Nishihara site. The distance from the surface fault to Nishihara is about 740 m, which is less than the size of sub-fault size (1,000 m). We also calculate the strong ground motion at 100m from the Futagawa fault, and investigate the fling step using two fault models. One is a model with a point source at the center of the sub-fault, and the other is an extended source model considering the effects of the fault plane.

Fig.6 shows the comparisons between the observed records (black lines) and the simulations (red lines) for the velocities (left) and displacements (right) at Mashiki and Nishihara. In the following figures, FP and FN stand for the componets of the fault parallel (N53E) and the normal (N143E), respectively. The simulated results reproduce well the recorded fling pulses in the velocities and the fling steps in the displacements at both sites. In addition, the contributions of the static and dynamic terms in the simulations are dipicted by the blue and green lines, respectively. Although the velocity pulses are the combination of the static and dynamic contributions, the fling step, as seen in the permanent offset in the displacements, are completely reproduced by the static contribution.

Finally, Fig.7 shows the comparisons of the results between the fault plane model and the point source model at Nishihara and the site of 100 m from the surface fault. Fig.7(a) shows the velocities is the displacements at Nishihara, the red lines represents the fault plane model, and the blue lines are the rsults by the point source model. Even though the distance from Nishihara to the Futagawa fault is about 740 m, and comparable to the fault size of 1km, the point source model underestimates the amplitude of the fling step. On the other hand, Fig.7(b) shows the result at 100m, which shows very large differences of resullts between the fault plane model and the point source model. Again, the point source model cannot reproduce accurate fling steps within the distance from the fault shorher than the sub-fault size.

4. Summary

Following Ref. [4], we demonstrated that "the fling step is the static contribution of Green's function", but not "the near-field term" or "the intermediate-field term" (*i.e.* Ref. [1], [2]). We also demonstrationed that our definition is valid for all types of underground structures using the examples of the simple circular fault model and the 2016 Kumamoto earthquake model. In addition, if the distance from the fault is very short (*i.e.* shorter than the radius for the circular fault model and the sub-fault size for the Kumamoto fault model), a point source model does not reproduce the fling step, and an extended source model must be used. We have made the Fortran codes for computing the fling step in layered half-space open to public use (http://kouzou.cc.kogakuin.ac.jp/Open/Green/).

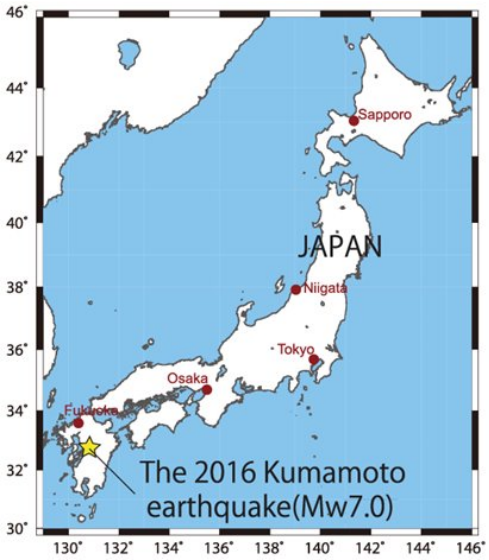

(a) The location of the 2016 Kumamoto eathqauke

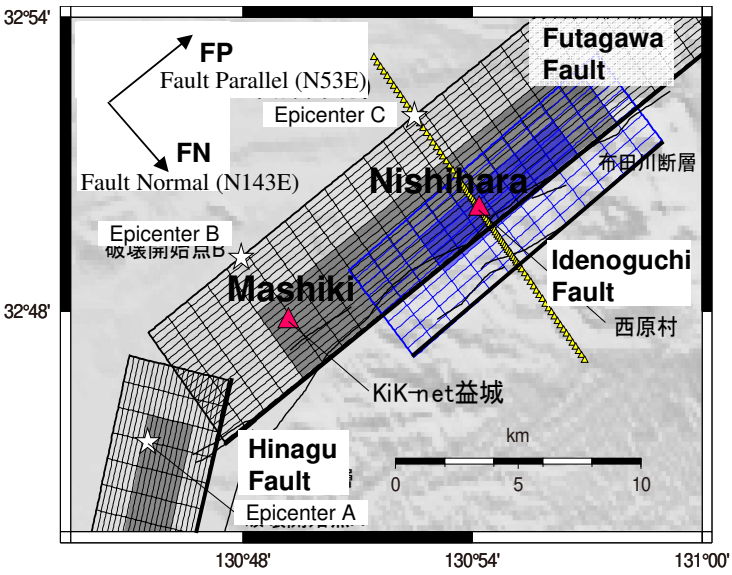

(b) The three faults (Futagawa, Hinagu, and Idenoguchi) and the two recording sites (Mashiki and Nishihara)

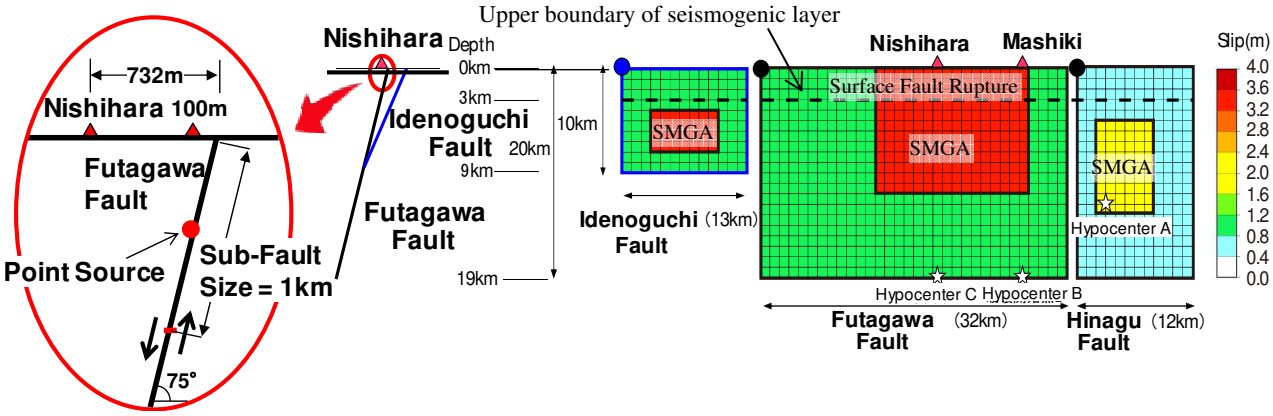

(c) (Right)The three fault models based on the recipe of predicting strong ground motions (Ref. [9]) below the seismogenic layer and the modified recipe considering the slower slip above the seismogenic layer (Ref. [8]), and (Left) the cross section including Nishihara and the two fault planes

Fig. 5 The three faults (the Futagawa, Hinagu, and Idenoguchi faults), and the two sites recorded the strong ground motion near the surface fault ruptures (Mashiki and Nishihara).

Table 1 Main fault parameters

Fault	Futagawa	Hinagu	Idenoguchi
L, W(km)	32, 20	12, 20	13, 10
sub-fault size	1 (km)		
strike (degree)	233	193	231
dip (degree)	75	78	65
rake (degree)	-160	-160	-135
slip (SMGA: m)	3.28	1.79	3.28
slip (back: m)	1.04	0.6	1.04

Table 2 Material properties of the layered half-space

Layer	density (t/m^3)	Vp (m/s)	Qp0	Vs (m/s)	Qs0	Thichness (m)
1	1.9	2000	100	600	100	3
2	2.15	2500	150	1100	150	147
3	2.4	4000	200	2100	200	487
4	2.6	5500	300	3100	300	1512
5	2.7	5700	300	3300	300	5000
6	2.75	6000	300	3400	300	-

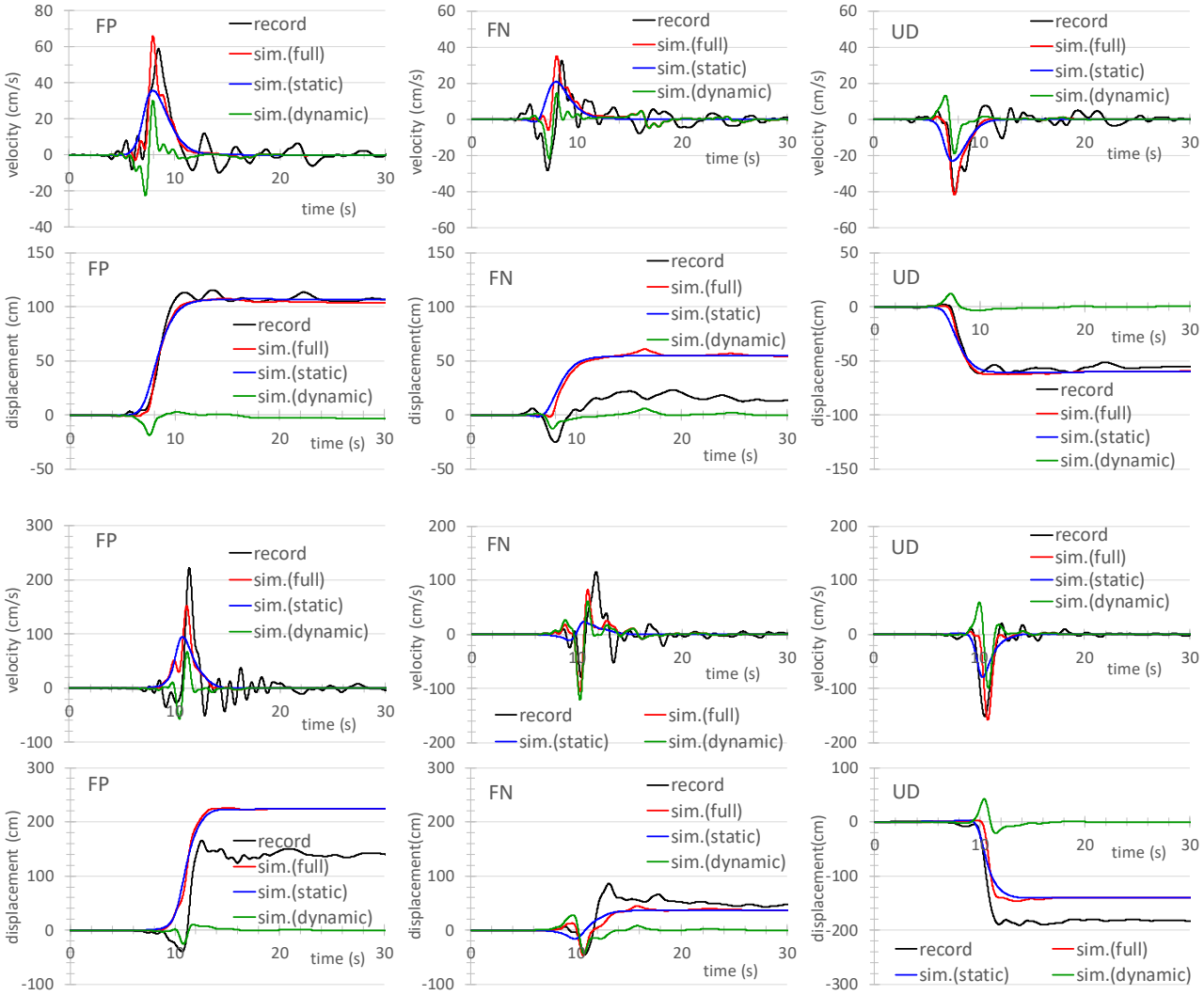

Fig. 6 The three seismic faults (Futagawa, Hinagu, and Idenoguchi Faults) and the two sites recording the strong ground motion near the surface fault ruptures (Mashiki and Nishihara).

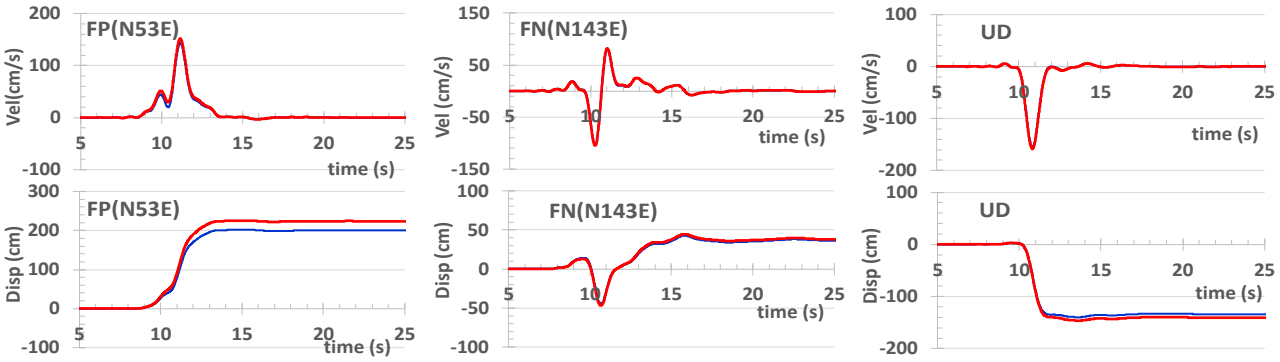

(a) Velocities (top) and displacement (bottom) at Nishihara (about 740 m from the Futagawa fault)

Fig. 7 Comparisons between the fault model (red lines) and the point source model (blue lines) at Nishihara and the 100 m sites from the Futagawa fault. "the point source model" is the model of a point source at the center of the sub-fault (1 km size), whereas "the fault model" is the model of the extended source model on the sub-faults subdevided considering the shortest distance from the fault.

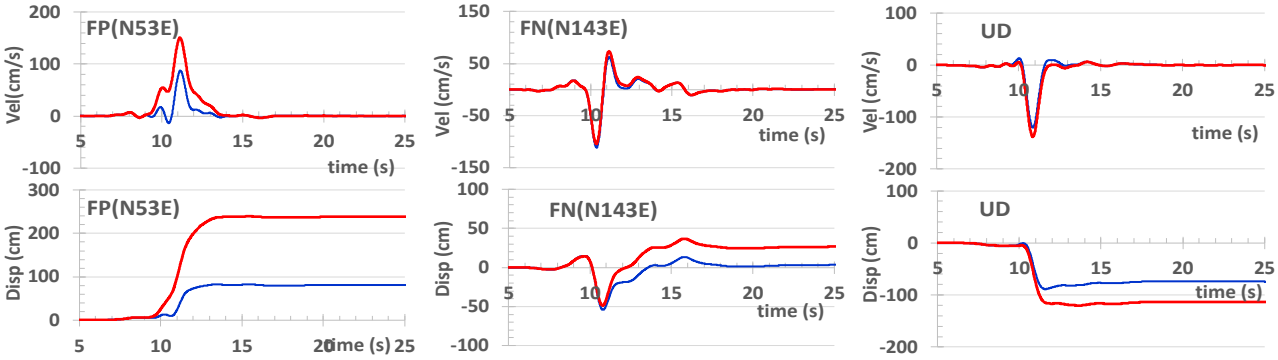

(b) Velocities (top) and displacement (bottom) at 100 m from the Futagawa fault

Fig. 7 (continued)

Acknowledgements

This study is partly supported by the Private University Research Branding Project of Research Institute of Kogakuin University and MEXT (Ministry of Education, Culture, Sports, Science and Technology). The strong motion records in Mashiki City and Nishihara Village were released by NIED (National Research Institute for Earth Science and Disaster Resilience), JMA (Japan Meteorological Agency), and Kumamoto Prefecture.

References

[1] Dreger D, Hurtado G, Chopra A, LarsenS (2011): Near-Field Across-Fault Seismic Ground Motions, *Bull. Seism. Soc. Am.*, **101**, 202–221.

[2] Koketsu K, Miyake H, Guo Y, Kobayashi H, Masuda T, Davuluri S, Bhattarai M, Adhikari LB, Sapkota SN (2016): Widespread ground motion distribution caused by rupture directivity during the 2015 Gorkha, Nepal earthquake, *Scientific Reports*, **6**, Article number: 28536.

[3] Aki K, Richards PG (1989): Quantitative Seismology: Theory and Methods, *W H Freeman & Co*.

[4] Hisada, Y, Bielak J (2003): A Theoretical Method for Computing Near-Fault Strong Motions in Layered Half-Space Considering Static Offset due to Surface Faulting, with a Physical Interpretation of Fling Step and Rupture Directivity, *Bull. Seism. Soc. Am.*, **93**, 1154-1168.

[5] Hisada Y (1994): An Efficient Method for Computing Green's Functions for a Layered Half-Space with Sources and Receivers at Close Depths, *Bull. Seism. Soc. Am.*, **84**, 1456-1472.

[6] Luco JE, Apsel RJ (1983): On the Green's functions for a layered haft-space, part 1, *Bull. Seism. Soc. Am.*, **73**, 909-929.

[7] Greenfield RJ (1995): Comment on "An efficient method for computing Green's functions for a layered half-space with sources and receivers at close depths" by Y.Hisada, *Bull. Seism. Soc. Am.* **85**, 1523-1524.

[8] Tanaka S, Kaneda J, Hikita K, Hisada Y (2018): Characterized fault model for prediction of long-period ground motions containing permanent displacement in the near-fault region, *J. Struct. Constr. Eng., Arch. Inst. Japan*, **83** (752), 1525-1535 (in Japanese).

[9] The Headquarters for Earthquake Research Promotion (2017): Strong ground motion prediction method for earthquakes with specified source faults ("Recipe") (in Japanese)

